Time Asymmetric Quantum Mechanics and Shock Waves: Exploring the Irreversibility in Nonlinear Optics

Giulia Marcucci, Maria Chiara Braidotti, Silvia Gentilini, and Claudio Conti*

The description of irreversible phenomena is a still debated topic in quantum mechanics. Still nowadays, there is no clear procedure to distinguish the coupling with external baths from the intrinsic irreversibility in isolated systems. In 1928 Gamow introduced states with exponentially decaying observables not belonging to the conventional Hilbert space. These states are named *Gamow vectors*, and they belong to rigged Hilbert spaces. This review summarizes the contemporary approach using Gamow vectors and rigged Hilbert space formalism as foundations of a generalized "time asymmetric" quantum mechanics. We study the irreversible propagation of specific wave packets and show that the topic is surprisingly related to the problem of irreversibility of shock waves in classical nonlinear evolution. We specifically consider the applications in the field of nonlinear optics. We show that it is possible to emulate irreversible quantum mechanical process by the nonlinear evolution of a laser beam and we provide experimental tests by the generation of dispersive shock waves in highly nonlocal regimes. We demonstrate experimentally the quantization of decay rates predicted by the time-asymmetric quantum mechanics. This work furnishes support to the idea of intrinsically irreversible wave propagation, and to novel tests of the foundations of quantum mechanics.

1. Introduction

Modifying the principles of quantum mechanics (QM) to explain time asymmetric (TA) phenomena is nowadays an open issue. A growing community of scientists is developing new models, theoretical tools and paradigms,[1–16] which are also proving to have intriguing applications in nonlinear physics and photonics.[17–20]

G. Marcucci, M. C. Braidotti, S. Gentilini, C. Conti
Institute for Complex Systems
National Research Council (ISC-CNR)
Via dei Taurini 19, 00185 Rome (IT)
E-mail: giulia.marcucci@uniroma1.it

G. Marcucci, C. Conti
Department of Physics
University Sapienza
Piazzale Aldo Moro 5, 00185 Rome (IT)

M. C. Braidotti
Department of Physical and Chemical Sciences
University of L'Aquila
Via Vetoio 10, I-67010 L'Aquila (IT)

The ORCID identification number(s) for the author(s) of this article can be found under https://doi.org/10.1002/andp.201600349

Generally, irreversible phenomena are described by exponentially decaying observables related to a determined arrow of time. However, this exponential dynamics is excluded from first principles in Hilbert space formulation of QM.[21–24] An evidence of this is the fact that damping is commonly introduced in a phenomenological way when accounting for the coupling with the environment.[9,15] Despite this, exponential decay of observable quantities is frequently detected in experiments, even when the role of the environment is negligible. This is called *the probability problem*, and it is common both to QM (particle decays), and classical systems[6] (nonlinear wave propagation).

In classical physics, in particular, there are various phenomena which theoretically can be reversible, but which do not show any experimental evidences about the possibility of inverting their dynamics, even when the coupling with environment is completely negligible, as illustrated in Refs. [25–31]. A paradigm of these are shock waves (SWs).

SWs are singular mathematical solutions of hyperbolic partial differential equations which presents a smooth trend until they reach the shock point. Then, in order to avoid a multivalued evolution, irregularities arise. More specifically, the shock point coincides with the gradient catastrophe or wave breaking (WB), i.e., an unbounded increase of a function partial derivative upon conditions of boundedness of the function itself.[32] In optics, the WB corresponds to a sudden change of the phase, while the intensity profile is regularized by the occurrence of fast oscillations, called *undular bores*. These undular bores cause a dispersion of light and, for this reason, the optical SWs are named *dispersive shock waves* (DSWs). One of the first detections of DSWs is reported in;[33] later many other physicists studied DSWs in optics, such as,[25,29,31,34,35] but no one demonstrated their reversibility experimentally.

The leading theoretical background of "time-asymmetric quantum-mechanics" (TA-QM) is the rigged Hilbert space (RHS): an enlarged Hilbert space that includes non-normalizable wave functions, which decay exponentially with respect to time. In this formalism, generalized eigenvalues with complex energies do have physical meaning,[36] and the corresponding non-normalizable eigenvectors called the Gamow vectors (GVs)[1,2] and form a numerable generalized basis for integrable functions. A paradigmatic model for TA-QM is the reversed harmonic

**ADVANCED
SCIENCE NEWS**

www.advancedsciencenews.com

annalen
der **physik**

www.ann-phys.org

oscillator (RHO), where this formalism allowed to find quantized decay rates obtained by writing the initial state in terms of a discrete summation of GVs. This surprizing quantization of decay rates has been experimentally observed in an optical emulation.[18]

In this manuscript, we review the basics of TA-QM and of the GVs approach to the RHO. Moreover, we study the way the function space of the input state has a direct counterpart in the long term evolution; in other words, we show that, depending on the initial shape of the wavefunction, one can have different long terms dynamics, as already shown in Ref. [16]. We consider the generation of spatial DSWs in nonlinear optical propagation as a specific example of a classical system which presents an inherently irreversible dynamics: as wrote before, in these regimes, singular solutions may be excited by smooth initial conditions that generate an evolution dominated by highly nonregular waves. Commonly adopted techniques in classical nonlinear field theory, like the Whitham approach, are limited to integrable or nearly integrable systems,[32,37] and cannot describe the global evolution of the wavepacket. Very simplified hydrodynamic models, like the Hopf equation, are used in most of the cases.[25,32,38,39] These methods allow the description of the wave propagation until the occurrence of the shock point, but do not provide a global and comprehensive analysis. On contrary, we show that GVs quantitatively describe DSWs and explain the observed exponential dynamics, as reported in Refs. [17–19]. This results demonstrate the way TA-QM is also relevant for important challenges of classical physics as the description of WB phenomena beyond the shock point. Importantly enough, we show that the link between TA-QM and SWs allows the first experimental demonstration of the quantization of decay-rates.[17]

This review was written for the purpose of displaying and collecting the theoretical and experimental works made by the authors on the description of DSWs by TA-QM. The most mathematical part, reported in Ref. [16], is summarized in the sections 2, 3 and 4, where we introduce the mathematical foundations of the TA-QM and define the RHS. The GVs and the RHO are described as well, addressing the way GVs intervene in modeling irreversible processes and providing RHO spectrum and properties. The theoretical part showing the link between nonlinear optics and TA-QM formalism, deepened in Ref. [17], is illustrated in the section 5 and explains the way GVs can be used to model nonlinear dispersive waves propagation in nonlocal nonlinear media. Finally, the last part concerns the experimental proofs, as reported in Refs. [18,19].

2. Mathematical Foundations of TA-QM

TA formulation of QM is founded on a specific mathematical background. In the following section, we explain a step by step procedure to obtain a standard QM on a Hilbert space $\mathcal{H}$ and the reason why we need to widen $\mathcal{H}$ in order to include non-normalizable states. We are going to use several tools typically ascribable to functional analysis and topology. Their mathematical definitions can be found in Appendix and in Refs. [40–43].

We start from a separable vector space Ψ, with a locally convex topology τ and a scalar product $(\cdot|\cdot)$. We need an algebra $\mathcal{A}$ of τ-continuous linear operator on Ψ and a probability measure $\mathcal{P}$

on $\mathcal{A}$. Thanks to the scalar product $(\cdot|\cdot)$, we get a norm $||\psi|| = \sqrt{(\psi|\psi)} \ \forall \psi \in \Psi$ and a metric $d(\psi, \phi) = ||\phi - \psi|| \ \forall \phi, \psi \in \Psi$, that is induced by the norm, and settle a new topology τ_d on Ψ, given by the distance d. In this way we find a Euclidean space (Ψ, τ_d), which is also normed and separable. To be a physical space, it needs the completeness. Let $(\mathcal{H}, \tau_{\mathcal{H}})$ be the completion of (Ψ, τ_d): $\mathcal{H}$ is the separable Hilbert space used to formulate the known time symmetric quantum theory. The following three theorems justify this last statement.

Theorem 2.1 Gleason. [21] *For every probability $\mathcal{P}(\Lambda)$, there exists a positive trace class operator ρ such that*

$$\mathcal{P}(\Lambda) = Tr(\Lambda \rho).$$

Theorem 2.2 Stone-Neumann. [22] *Let us consider the Schrödinger-Neumann equation for ρ previously defined*

$$\frac{\partial \rho(t)}{\partial t} = \frac{i}{\hbar}[H, \rho(t)],$$

with H Hamiltonian operator. The solutions of such an equation are time symmetric and they are given by the group of unitary operators $U^\dagger(t) = \exp{-\frac{i}{\hbar} Ht}$.

Theorem 2.3 Hegerfeldt. [23] *For every Hermitian and semi-bounded Hamiltonian H, either*

$$Tr(\Lambda(t)\rho) = Tr(\Lambda \rho(t)) = 0 \ \forall t \in \mathbb{R}$$

or

$$Tr(\Lambda(t)\rho) = Tr(\Lambda \rho(t)) > 0 \ \forall t \in \mathbb{R}$$

except on a set of Lebesgue measure zero.

These theorems imply that time asymmetric solutions of the Schrödinger equation $i\hbar\frac{\partial \phi(t)}{\partial t} = H\phi(t)$ with time asymmetric boundary conditions are not allowed, hence we need to modify the mathematical description of the system.

For every fixed $\psi_0 \in \Psi$, the translation $T : \Psi \to \Psi$ such that $\psi \to \psi + \psi_0$ is a linear homeomorphism of Ψ on itself. Therefore τ is uniquely determined by the neighborhood system $I(0)$ centered at the origin, because every other neighborhood of any point ψ of Ψ is obtained by translating a neighborhood of the origin of the vector ψ. (Ψ, τ) is said to be locally convex if $\mathcal{C} = \{C \in I(0) \ | \ C$ is convex$\}$ is a neighborhood local basis. Since every open ball $B_r(x_0) = \{x \in X \ | \ d(x_0, x) < r\}$ is convex, it is also a member of $\mathcal{C}$ if and only if $\exists A \in \tau \ | \ 0 \in A \subset B_r(0) \ \forall B_r(0)$. By this last condition, we build a locally convex topology τ on Ψ that is finer than the topology τ_d induced by the norm.

Let us suppose that (Ψ, τ) and $(\mathcal{H}, \tau_{\mathcal{H}})$ are the previously described spaces and, besides, τ is locally convex and finer than $\tau_{\mathcal{H}}$. Then we can define another completion Φ of Ψ, this time with respect to τ, and find another complete space (Φ, τ_Φ) that is different from $(\mathcal{H}, \tau_{\mathcal{H}})$. Precisely, $\Phi \subset \mathcal{H}$, and Φ is dense in $\mathcal{H}$. Moreover, $\Phi \subset \mathcal{H} \Rightarrow \mathcal{H}^* \subset \Phi^*$, where $\mathcal{H}^*$ and Φ^* are the dual spaces of $\mathcal{H}$ and Φ, respectively. The definition of dual space is the basis to build a RHS and we need a more physically accessible dual space, according to Refs. [4,5,8–10]. Let $\mathcal{E}$ be a Euclidean space.

**ADVANCED
SCIENCE NEWS**

www.advancedsciencenews.com

annalen
der **physik**

www.ann-phys.org

We identify the scalar product on $\mathcal{E}$ as $(\cdot|\cdot)$; instead $\langle\cdot|\cdot\rangle$ is the operatorial product on the dual space $\mathcal{E}^*$, namely $F(v) = \langle F|v\rangle$. We define our dual space $\Phi^\times$ as the space of *antilinear* and continuous functionals on Φ, that is $F \in \Phi^\times \iff F(\phi) = \langle\phi|F\rangle$. Thus every functional in $\Phi^\times$ has a sort of complex conjugate in Φ^*, and the Riesz-Frechet[40] representation theorem on the Hilbert space $\mathcal{H}$ still works, hence $\mathcal{H} = \mathcal{H}^\times$. In this manner we obtain the *Gelfand triplet* $\Phi \subset \mathcal{H} \subset \Phi^\times$, which defines our RHS.

3. Gamow Vectors

The Hamiltonian operator H of a quantum system must be self-adjoint on the Hilbert space $\mathcal{H}$ in order to be observable, so $H = H^\dagger$. Nevertheless $H \neq H^\times$ on $\Phi^\times$. In fact, we identify with $H^\dagger$ the adjoint on $\mathcal{H}$ of H, while $H^\times$ represents the adjoint on $\Phi^\times$ of H restricted to Φ. In other word, in the first case we have that $\mathcal{H} = \mathcal{H}^\times$ implies $H = H^\dagger$; in the second case, we have $H : \Phi \to \Phi$ and $H^\times : \Phi^\times \to \Phi^\times$ with $\Phi \neq \Phi^\times$, hence they must be different. Let us consider the secular equation

$$H^\times|E\rangle = E|E\rangle. \tag{1}$$

If $|E\rangle \in \Phi^\times \setminus \mathcal{H}$, we cannot affirm that the corresponding eigenvalue E is a real number. We define a generalized eigenvector $|E\rangle \in \Phi^\times$, which has complex eigenvalue, as a *Gamow vector* $|\phi^G\rangle = |E^\pm\rangle = |E^R \pm i\frac{\Gamma}{2}\rangle$, $\Gamma \geq 0$ (apex R is due to one of the first applications of this theory, that Bohm developed in scattering experiments,[4] and it is related to the resonances of the system). From the Schrödinger equation (in units such that $\hbar = 1$), we get a unitary operator $U(t) = e^{-iHt}$ for the temporal evolution of any state in $\mathcal{H}$. We see that $U(t)^\times = e^{iH^\times t}$ is not unitary on $\Phi^\times$:

$$U(t)^\times \left|E^R \pm i\frac{\Gamma}{2}\right\rangle = e^{iE^R t} e^{\mp\frac{\Gamma}{2}t} \left|E^R \pm i\frac{\Gamma}{2}\right\rangle, \tag{2}$$

$U(t)^\times$ is not an isometry, because

$$\left\|U(t)^\times \left|E^R \pm i\frac{\Gamma}{2}\right\rangle\right\|^2 = e^{\mp\Gamma t} \left\|\left|E^R \pm i\frac{\Gamma_n}{2}\right\rangle\right\|^2. \tag{3}$$

Moreover

$$\left\|U(t)^\times \left|E^R \pm i\frac{\Gamma}{2}\right\rangle\right\| \xrightarrow{t\to\pm\infty} 0 \tag{4}$$

and

$$\left\|U(t)^\times \left|E^R \pm i\frac{\Gamma}{2}\right\rangle\right\| \xrightarrow{t\to\mp\infty} +\infty. \tag{5}$$

We identify Φ with the Schwartz space $S(\mathbb{R}^N)$, that is, the space of rapidly decreasing functions, and the Hilbert space $\mathcal{H}$ with the space of quadratically integrable functions $\mathcal{L}^2(\mathbb{R}^N)$, commonly used in quantum systems. We define the following new spaces:

$$\Phi_- = \left\{\phi \in \Phi \mid f(E) = \langle\phi|E^-\rangle \in S(\mathbb{R}) \cap \mathcal{H}_-^2\right\},$$

$$\Phi_+ = \left\{\phi \in \Phi \mid f(E) = \langle\phi|E^+\rangle \in S(\mathbb{R}) \cap \mathcal{H}_+^2\right\},$$

where $\mathcal{H}_-^2$ ($\mathcal{H}_+^2$) is the Hardy space for the lower (upper) complex half plane. To sum up, $\Phi_\pm$ are dense in Φ, $\Phi = \Phi_- + \Phi_+$ ($\Phi_- \cap \Phi_+ \neq 0$ generally) and Φ is dense in $\mathcal{H}$, consequently

$$\Phi_- \overset{dense}{\subset} \Phi \overset{dense}{\subset} \mathcal{H} \overset{dense}{\subset} \Phi^\times \overset{dense}{\subset} \Phi_-^\times, \tag{6}$$

$$\Phi_+ \overset{dense}{\subset} \Phi \overset{dense}{\subset} \mathcal{H} \overset{dense}{\subset} \Phi^\times \overset{dense}{\subset} \Phi_+^\times. \tag{7}$$

We have now found two Gelfand triplets, $\Phi_- \subset \mathcal{H} \subset \Phi_-^\times$ and $\Phi_+ \subset \mathcal{H} \subset \Phi_+^\times$, where the evolution operator $U(t)$ acts as a semigroup, because it is well defined and continuous only for $t \leq 0$ on Φ_-, and only for $t \geq 0$ on Φ_+.

In the following, we show in detail the way the passage from a standard separable Hilbert space to a RHS affects the dynamics through a simple model: the damped motion. We consider the classical dynamical system in one dimension

$$\begin{cases} \frac{d}{dt}u(t) = -\gamma u(t) \\ u(0) = u_0 \end{cases} \tag{8}$$

where $\gamma > 0$ and $m = \hbar = 1$. We have $u(t) = e^{-\gamma t}u_0$, which represents a damping for $t \geq 0$. We can quantize it, even if this one is not a Hamiltonian system, and we get[13]

$$\hat{H}(\hat{u}, \hat{v}) = -\frac{\gamma}{2}(\hat{u}\hat{v} + \hat{v}\hat{u}). \tag{9}$$

By performing the canonical transformation

$$\hat{u} = \frac{\gamma\hat{x} - \hat{p}}{\sqrt{2\gamma}}, \quad \hat{v} = \frac{\gamma\hat{x} + \hat{p}}{\sqrt{2\gamma}}, \tag{10}$$

one obtains the Hamiltonian of the Reversed Harmonic Oscillator (RHO):

$$\hat{H}(\hat{x}, \hat{p}) = \frac{\hat{p}^2}{2} - \frac{\gamma^2\hat{x}^2}{2}. \tag{11}$$

As proved in Ref. [13], $\hat{H}(\hat{u}, \hat{v})$ is self-adjoint on $\mathcal{L}^2(\mathbb{R})$ and parity invariant. We define the time reversal operator T such that

$$T\phi(t) := \phi(-t) \Rightarrow TU(t) = U^\dagger(t)T \Rightarrow U(t)TU(t) = T,$$

where $U(t) := e^{-iHt}$. T plays a fundamental role in this system, and coincides with the inverse Fourier transformation, i.e. $T\phi(u, t) := \check{F}[\phi](u, t)$, where $\check{F}[\phi](x, t) = \frac{1}{\sqrt{2\pi}}\int_\mathbb{R} e^{ikx}\phi(k, t)dk$.

Let us define two families of tempered distributions in $\Phi^\times$, the first one

$$\hat{u}\left|f_0^-\right\rangle := 0, \quad f_0^-(u) = \delta(u), \quad \left|f_n^-\right\rangle := \frac{(-i)^n}{\sqrt{n!}}\hat{v}^n\left|f_0^-\right\rangle \tag{12}$$

$$\Rightarrow f_n^-(u) = \frac{(-1)^n}{\sqrt{n!}}\frac{d^n}{du^n}\delta(u) \quad \forall n \in \mathbb{N}; \tag{13}$$

and the second one

$$\hat{v}\,|f_0^+\rangle := 0, \quad f_0^+(u) = 1, \quad |f_n^+\rangle := \frac{1}{\sqrt{n!}}\hat{u}^n\,|f_0^+\rangle \tag{14}$$

$$\Rightarrow \quad f_n^+(u) = \frac{u^n}{\sqrt{n!}} \quad \forall n \in \mathbb{N}. \tag{15}$$

Hereafter, following,[4,5,8–10] we denote a tempered distribution $f_n^{\pm}$ a *resonance*. We can see that $H^{\times}|f_n^{\pm}\rangle = \pm E_n|f_n^{\pm}\rangle$, where $E_n := i\gamma(n + \frac{1}{2}) \in \mathbb{C}$. Given that $f_n^{\pm}$ are tempered distributions, their inverse Fourier transforms are well defined, and they are

$$\check{F}\left[f_n^-\right] = \frac{i^n}{\sqrt{2\pi}}f_n^+, \tag{16}$$

$$\check{F}\left[f_n^+\right] = i^n\sqrt{2\pi}f_n^-. \tag{17}$$

One may see that the resonances are *quasi-orthogonal* and *quasi-complete*, namely,

$$\langle f_n^-|f_m^+\rangle = \delta_{n,m}$$

and

$$\sum_{n=0}^{\infty} f_n^-(u)f_n^+(\gamma) = \delta(u - \gamma),$$

respectively.

In order to find real energy values, we need to analyze also the continuous spectrum. Since H is parity invariant, each generalized eigenvalue is doubly degenerate, thus $H^{\times}\psi_{\pm}^E = E\psi_{\pm}^E$. As one can see in Ref. [13], the generalized eigenfunctions are

$$\psi_{\pm}^E(u) = \frac{1}{\sqrt{2\pi\gamma}}u_{\pm}^{-\left(\frac{iE}{\gamma}+\frac{1}{2}\right)}, \tag{18}$$

where $u_{\pm}^{\lambda}$ are tempered distributions such that

$$u_+^{\lambda} := \begin{cases} u^{\lambda} & u \geq 0 \\ 0 & u < 0 \end{cases}, \quad u_-^{\lambda} := \begin{cases} 0 & u < 0 \\ u^{\lambda} & u \leq 0 \end{cases}.$$

It is possible to prove both the orthonormality and the completeness of the eigenfunctions, namely,

$$\sum_{\pm} \int \left[\psi_{\pm}^{E_1}(u)\right]^* \psi_{\pm}^{E_2}(u)\,du = \delta(E_1 - E_2)$$

and

$$\sum_{\pm} \int \left[\psi_{\pm}^E(u)\right]^* \psi_{\pm}^E(u')\,dE = \delta(u - u').$$

Therefore we can apply the Gelfand-Maurin theorem[44] and write any function in $S(\mathbb{R})$ as

$$\phi(u) = \sum_{\pm} \int \psi_{\pm}^E(u)\langle\phi|\psi_{\pm}^E\rangle^*\,dE.$$

By repeating the same reasoning

$$H^{\times}\check{F}\left[\psi_{\pm}^{-E}\right] = E\check{F}\left[\psi_{\pm}^{-E}\right], \tag{19}$$

so one can prove also the orthonormality and the completeness of the inverse Fourier transforms of the eigenfunctions, whence

$$\phi(u) = \sum_{\pm} \int \check{F}\left[\psi_{\pm}^{-E}\right](u)\langle\phi|\check{F}\left[\psi_{\pm}^{-E}\right]\rangle^*\,dE. \tag{20}$$

We have just defined two groups of eigenfunctions, $\psi_{\pm}^E(u)$ and $\check{F}[\psi_{\pm}^{-E}](u)$, which represent the continuous spectrum of the Hamiltonian of a damped motion into the RHS. Moreover, we have just seen that they depend on the tempered distributions $u_{\pm}^{-\left(\frac{iE}{\gamma}+\frac{1}{2}\right)}$, which have simple poles in the complex plane when $E = -E_n = -i\gamma(n + \frac{1}{2})$. Thanks to the properties of the generalized function $u_{\pm}^{\lambda}$,[13] we can finally state what follows:

$$Res\left[\psi_{\pm}^E, -E_n\right] = \frac{(\pm 1)^n i\sqrt{\gamma}}{\sqrt{2\pi n!}}f_n^-, \tag{21}$$

$$Res\left[\check{F}\left[\psi_{\pm}^{-E}\right], E_n\right] = \frac{(\pm i)^n i\sqrt{\gamma}}{2\pi\sqrt{n!}}f_n^+. \tag{22}$$

By defining the following spaces, we get two Gelfand triplets: $\mathcal{H} = \mathcal{L}^2(\mathbb{R}), \Phi = S(\mathbb{R})$,

$$\Phi_- = \left\{\phi \in \Phi \mid f(E) = \langle\phi|\check{F}\left[\psi_{\pm}^{-E}\right]\rangle \in \mathcal{H}_-^2\right\}, \tag{23}$$

$$\Phi_+ = \left\{\phi \in \Phi \mid f(E) = \langle\phi|\psi_{\pm}^E\rangle \in \mathcal{H}_+^2\right\}. \tag{24}$$

From this framework into the RHS $\Phi^{\times}$, we can infer the irreversible evolution of certain waves in Φ. We established above the connection between the continuous and the point spectrum. Now we make this link definitively clear and we show that the evolution operator acts as a semigroup on $\Phi_{\pm}$ for a well-defined orientation of the arrow of time. By recalling Eqs.(21) and (22), we apply the residue theorem to initial data in $\Phi_{\pm}$[13] and get two different expansions in GVs:

$$\phi^+(u) = \sum_{n=0}^{+\infty} \langle\phi^+|f_n^+\rangle f_n^-(u) \quad \forall \phi^+ \in \Phi_+; \tag{25}$$

$$\phi^-(u) = \sum_{n=0}^{+\infty} \langle\phi^-|f_n^-\rangle f_n^+(u) \quad \forall \phi^- \in \Phi_-. \tag{26}$$

Thanks to the following definitions of two new function spaces, both of them subspaces of $S(\mathbb{R})$ and isomorphic by the inverse Fourier transformation, we can establish the relation between Φ_+ and Φ_-: $\mathcal{D} = C_c^{\infty}(\mathbb{R})$ is the space of the infinitely differentiable functions with compact support; $\mathcal{Z} = \left\{\check{F}[\phi] \mid \phi \in \mathcal{D}\right\}$, where $\check{F}$ is the inverse Fourier transformation.
For each function $\phi \in \mathcal{Z}$ we have

$$\phi(u) = \sum_{n=0}^{+\infty} \frac{1}{n!}\frac{d^n}{du^n}\phi(u)|_{u=0}u^n = \sum_{n=0}^{+\infty} f_n^+(u)\langle f_n^-|\phi\rangle,$$

**ADVANCED
SCIENCE NEWS**

www.advancedsciencenews.com

annalen
der **physik**

www.ann-phys.org

while, at the same time, every $\psi \in \mathcal{D}$ is the Fourier transform of a function in $\mathcal{Z}$, hence

$$\psi(u) = \frac{1}{\sqrt{2\pi}} \int_{\mathbb{R}} \check{F}[\psi](v) e^{-ivu} dv = \sum_{n=0}^{+\infty} f_n^-(u) \left\langle f_n^+ | \psi \right\rangle .$$

Then we can state that

$$\Phi_+ \equiv \mathcal{D}, \quad \Phi_- \equiv \mathcal{Z}. \tag{27}$$

At last, we study the evolution operator $U(t) = e^{-iHt}$. U is a unitary group on $\mathcal{H} = \mathcal{L}^2(\mathbb{R})$, given that if
$\psi(u, 0) \in \mathcal{L}^2(\mathbb{R})$ then

$$\psi(u, t) = U(t) \psi(u, 0) = e^{\frac{\gamma}{2} t} \psi \left(e^{\gamma t} u, 0 \right) , \tag{28}$$

transformation that turns out to be an isometry on $\mathcal{L}^2(\mathbb{R})$. This means that if $\psi(u, t)$ solves the Schrödinger equation, then also $T\psi(u, t) = \psi(u, -t)$ does. Therefore the theory is time-reversal invariant on the Hilbert space $\mathcal{H}$, without letting us see the damping we expected. Where do we observe the temporal irreversibility? It lacks the analysis of U restricted to $\Phi_\pm$. If $\phi^+(u, 0) \in \Phi_+$ then

$$\left\langle U(t)\phi^+ | \psi_\pm^E \right\rangle = \left\langle \phi^+ | U^\times(t) \psi_\pm^E \right\rangle = e^{iEt} \left\langle \phi^+ | \psi_\pm^E \right\rangle \in \mathcal{H}_+^2$$

if and only if $t \geq 0$. On the other hand, if $\phi^-(u, 0) \in \Phi_-$ then

$$\left\langle U(t)\phi^- | \check{F}[\psi_\pm^{-E}] \right\rangle = \left\langle U(-t) \check{F}[\phi^-] | \psi_\pm^{-E} \right\rangle$$

$$= \left\langle \check{F}[\phi^+] | U^\times(-t) \psi_\pm^{-E} \right\rangle = e^{iEt} \left\langle \check{F}[\phi^-] | \psi_\pm^{-E} \right\rangle$$

$$= e^{iEt} \left\langle \phi^- | \check{F}\left[\psi_\pm^{-E}\right] \right\rangle \in \mathcal{H}_-^2$$

if and only if $t \leq 0$. We conclude that $U(t)$ establishes two semigroups:

$$U_+(t) : \Phi_+ \longrightarrow \Phi_+ \quad \forall t \geq 0$$

and

$$U_-(t) : \Phi_- \longrightarrow \Phi_- \quad \forall t \leq 0.$$

We have just found a way to model irreversible phenomena. In fact, the action of U allows to choose an orientation of the temporal arrow: if it goes forward from zero, then our initial data is in Φ_+, otherwise it is in Φ_-, indeed

$$\phi^+(u, t) = \sum_n e^{-\gamma(n+1/2)t} \left\langle \phi^+ | f_n^+ \right\rangle f_n^-(u) \tag{29}$$

and

$$\phi^-(u, t) = \sum_n e^{\gamma(n+1/2)t} \left\langle \phi^- | f_n^- \right\rangle f_n^+(u). \tag{30}$$

Moreover, all the physics we get fixing a specific orientation of time's arrow is achievable fixing the other one too, because time reversal operator T establishes an isomorphism between Φ_+ and Φ_-, that is, $T\phi^+(u, t) = U(-t) T\phi^+(u, 0) = \phi^-(u, -t)$.

Summarizing, we got an irreversible quantum system by observing that the evolution operator acts as a semigroup on $\Phi_\pm$, due to the presence of resonant states $f_n^\pm$. In this way, the instant $t = 0$ separates the evolution in two complementary directions: if one starts from Φ_+, one can stays forever in Φ_+ only evolving forward in time. In other words one chooses the temporal orientation, fixes the signature of $\Phi_\pm$, and cannot go backwards.

A last intriguing question is still unanswered: if we consider an initial wavefunction $\phi(u)$ which does not belong neither to $\mathcal{D}$ nor to $\mathcal{Z}$, such as the Gaussian function, and we let it evolve under the action of $U(t)$ for $t \geq 0$, what happens? In such a case, we cannot apply the residue theorem, and so we cannot derive an expression as the equation (25), because we have no hypothesis on the convergence of the series. Therefore, we need to truncate the summation and to define the N-order *background function* as

$$\phi_N^{BG}(u, t) := \phi(u, t) - \sum_{n=0}^{N} f_n^-(u) \left\langle U(t)\phi \, | \, f_n^+ \right\rangle^* \in \Phi^\times.$$

Consequently

$$\phi(u, t) = \sum_{n=0}^{N} f_n^-(u) \left\langle U(t)\phi \, | \, f_n^+ \right\rangle^* + \phi_N^{BG}(u, t) \quad \forall \phi \in \Phi.$$

For $\phi \in \Phi_+$, $\phi_{N \to +\infty}^{BG} = 0$, $U(t)$ acts as a semigroup and the evolution is a superposition of exponentially decaying functions. On the contrary, for $\phi \notin \Phi_+$, $\phi_{N \to +\infty}^{BG}$ does not converge and the evolution includes components which decay algebraically. For more details about the dependence of the evolution on the choice of the initial datum, one may refer to Ref. [16].

4. The Reversed Harmonic Oscillator

It is well known that the Harmonic Oscillator (HO) models the behavior of a pointlike mass around a stable equilibrium. If one overturns the HO potential, then one gets a parabolic barrier called the RHO, which gives the dynamics around an unstable equilibrium, an intrinsically irreversible evolution. We saw in Sec. 3 that it is possible to move from the damped motion Hamiltonian to the RHO one by a canonical transformation, hence we expect they hold two linked spectra into the RHS. At the same time, understanding the mathematical connections between the HO and the RHO is interesting, since we pass from the first Hamiltonian to the second one only by changing the real frequency ω into the complex value $i\gamma$,[45] as will be clear soon.

The classical HO Hamiltonian is $H = \frac{p^2}{2m} + \frac{m\omega^2}{2} x^2$. We quantize the HO by converting the canonical coordinates x, p into the operators $\hat{x}$, $\hat{p}$ such that $[\hat{x}, \hat{p}] = i\hbar$, and we find the spectrum of H:

$$H\psi(x) = E\psi(x), \quad E_n = \hbar\omega \left(n + \frac{1}{2} \right),$$
$$\psi_n(x) = \sqrt[4]{\frac{m\omega}{\hbar\pi}} \frac{1}{\sqrt{2^n n!}} H_n \left(\sqrt{\frac{m\omega}{\hbar}} x \right), \tag{31}$$

where $H_n(x) = (-1)^n x^2 \frac{d^n}{dx^n} e^{-x^2}$ are the Hermite polynomials.

We consider the family of operators[14]

$$\hat{V}_\lambda = \exp\left\{\frac{\lambda}{2}(\hat{x}\hat{p} + \hat{p}\hat{x})\right\}.$$

In a system of measurement where $\hbar = 1$, we have $[\hat{x}, \hat{p}] = i$, so $\hat{V}_\lambda \phi(x) = e^{-i\frac{\lambda}{2}}\phi(e^{-i\lambda}x)$, whence $\hat{V}_\lambda \hat{x}\hat{V}_\lambda^{-1} = e^{-i\lambda}\hat{x}$ and $\hat{V}_\lambda \hat{p}\hat{V}_\lambda^{-1} = e^{i\lambda}\hat{p}$. It is easy to see that $\hat{V}_{\pm\frac{\pi}{4}} H \hat{V}_{\pm\frac{\pi}{4}}^{-1} = \pm i\, H_{HO}$, hence we can transform the results we already know for the HO in results for the RHO:

$$E_n^{HO} = \gamma\left(n + \frac{1}{2}\right), \quad E_n = i\, E_n^{HO} \in \mathbb{C}$$

$$\psi_n^{HO} = \left(\frac{\gamma}{\pi}\right)^{1/4} (2^n n!)^{-1/2} e^{-\frac{\gamma}{2}x^2} H_n(\sqrt{\gamma}x)$$

$$\mathfrak{f}_n^\pm = \hat{V}_{\pm\frac{\pi}{4}}^{-1}\psi_n^{HO} \in S^\times(\mathbb{R}).$$

One passes from the HO to the RHO through the operator $\hat{V}_{\pm\frac{\pi}{4}}$, but can also pass from $H(\hat{u}, \hat{v})$ to $H(\hat{x}, \hat{p})$, i.e., from the damped motion to the RHO, by a canonical transformation and find a relation between the spectra of these two Hamiltonians. The canonical transformation from (u, v) to (x, p) it is generated by the generating function

$$S(x, u) = \frac{\gamma}{2}x^2 - \sqrt{2\gamma}xu + \frac{1}{2}u^2, \tag{32}$$

with $p = \frac{\partial S}{\partial x}$, $v = -\frac{\partial S}{\partial u}$. We define the unitary transformation

$$\mathcal{U} : \mathcal{L}^2(\mathbb{R}) \longrightarrow \mathcal{L}^2(\mathbb{R}) \tag{33}$$

such that $f(u) \longrightarrow (\mathcal{U}f)(x) = \tilde{C}\int_\mathbb{R} f(u)e^{iS(x,u)}du$, with $\tilde{C} := e^{-i\frac{\pi}{8}}\sqrt[4]{\frac{\gamma}{2\pi^2}}$ and we can prove that $\mathcal{U}$ is unitary by demonstrating that $|\tilde{C}|^2 \int_\mathbb{R} e^{i[S(x,u)-S(x',u)]}du = \delta(x - x')$.

In order to get a relation of quasi-orthogonality and quasi-completeness for the resonances, we need to understand the nature of the operator $\hat{V}_\lambda$. It acts almost like the evolution operator U in Eq. (28), with a complex (instead of real) exponential, but this is enough only to say that $\hat{V}_\lambda$ is unitary for pure imaginary λ, not for every $\lambda \in \mathbb{C}$. In fact, for a generic $\lambda = \omega + i\gamma$, where $\omega, \gamma \in \mathbb{R}$, one has

$$\langle \hat{V}_\lambda \phi | \hat{V}_\lambda \psi \rangle = \int_\mathbb{R} dx \left[e^{\frac{\gamma - i\omega}{2}}\phi\left(e^{\gamma - i\omega}x\right) \right]^* e^{\frac{\gamma - i\omega}{2}}\psi\left(e^{\gamma - i\omega}x\right) =$$

$$= e^{i\omega}\int_\mathbb{R} dx\, [\phi(x)]^*\psi(x) = e^{i\omega}\langle \phi | \psi \rangle.$$

Therefore it is not surprising that $\mathfrak{f}_n^\pm$ are only proportional to $\mathcal{U}[f_n^\pm(u)](x)$ and not exactly equal. In fact

$$\mathfrak{f}_n^\pm(x) = e^{in\frac{\pi}{4}}(2\pi)^{\pm\frac{1}{4}}\mathcal{U}\left[f_n^\pm(u)\right](x).$$

Nevertheless, we achieve the same relation of quasi-orthogonality and quasi-completeness we had before: $\langle \mathfrak{f}_n^\pm | \mathfrak{f}_m^\mp \rangle = \delta_{nm}$; $\sum_{n=0}^{+\infty}[\mathfrak{f}_n^\pm(x)]^*\mathfrak{f}_n^\mp(x') = \delta(x - x')$. Moreover $[\mathfrak{f}_n^\pm(x)]^* = \mathfrak{f}_n^\mp(x)$. Recalling the equations (16), (17) and the meaning of the inverse Fourier transform for the damped motion represented by

$\hat{H}(\hat{u}, \hat{v})$ (the inverse Fourier transform coincides with the time reversal operator T in that system), one has $T = C$, where C is the complex conjugation operator, as shown in Ref. [14].

From Ref. [14], we get the complete derivation of $\chi_\pm^E$, $\eta_\pm^E$ such that $H\chi_\pm^E = E\chi_\pm^E$, $H\eta_\pm^E = -E\eta_\pm^E$, respectively. We observe that $\eta_\pm^E(x) = [\chi_\pm^E(x)]^*$, fact which confirms that the time reversal operator T acts like the complex conjugation C. Moreover, from the corresponding properties satisfied by $\psi_\pm^E(u)$ and from the unitary nature of $\mathcal{U}$, we have $\sum_\pm \int_\mathbb{R} [\chi_\pm^E(x)]^*\chi_\pm^{E'}(x)dx = \delta(E - E')$, $\sum_\pm \int_\mathbb{R} [\chi_\pm^E(x)]^*\chi_\pm^E(x')dE = \delta(x - x')$, and the same results for $\eta_\pm^E(x)$.

At this point, we have got all the tools we need to study the analytic properties of these four families of eigenfunctions. The outcome is that $\chi_\pm^E(x)$ and $\eta_\pm^E(x)$ have simple poles at $E = -E_n$ and $E = E_n$, respectively. Furthermore,

$$Res\left[\chi_\pm^E(x); -E_n\right] \propto \mathfrak{f}_n^+(x), \tag{34}$$

$$Res\left[\eta_\pm^E(x); E_n\right] \propto \mathfrak{f}_n^-(x). \tag{35}$$

Following section 3, we get $\Phi_\pm$ from the residues of the RHO eigenfunctions:

$$\mathcal{H} = \mathcal{L}^2(\mathbb{R}), \quad \Phi = S(\mathbb{R}),$$

$$\Phi_- = \left\{\phi \in \Phi \mid f(E) = \langle \phi | \eta_\pm^E \rangle \in \mathcal{H}_-^2\right\},$$

$$\Phi_+ = \left\{\phi \in \Phi \mid f(E) = \langle \phi | \chi_\pm^E \rangle \in \mathcal{H}_+^2\right\},$$

with $T = C$ and $T(\Phi_+) = \Phi_-$. We study waves $\phi_\pm \in \Phi_\pm$ and the action of the evolution operator. Thanks to the Gelfand-Maurin spectral theorem

$$\phi^+(x) = \sum_\pm \int_\mathbb{R} dE\, \chi_\pm^E(x)\langle \phi^+ | \psi_\pm^E \rangle^* \tag{36}$$

and

$$\phi^-(x) = \sum_\pm \int_\mathbb{R} dE\, \eta_\pm^E(x)\langle \phi^- | \eta_\pm^E \rangle^*, \tag{37}$$

thus we are allowed to write the envelopes of $\phi_\pm$ in series of resonances:

$$\phi^+(x) = \sum_{n=0}^{+\infty}\langle \phi^+ | \mathfrak{f}_n^+ \rangle^* \mathfrak{f}_n^-(x) \quad \forall\, \phi^+ \in \Phi_+;$$

$$\phi^-(x) = \sum_{n=0}^{+\infty}\langle \phi^- | \mathfrak{f}_n^- \rangle^* \mathfrak{f}_n^+(x) \quad \forall\, \phi^- \in \Phi_-.$$

In conclusion, even in this case, the temporal evolution operator $U(t) = e^{-iHt}$ establishes a unitary group on $\mathcal{H} = \mathcal{L}^2(\mathbb{R})$, and two semigroups:

$$U_+(t) : \Phi_+ \longrightarrow \Phi_+ \quad \forall t \geq 0; \quad U_-(t) : \Phi_- \longrightarrow \Phi_- \quad \forall t \leq 0.$$

Furthermore, if $\phi^+(x, 0) \in \Phi_+$ then

$$\phi^+(x, t) = \sum_n e^{-\gamma(n+1/2)t}\langle \phi^+ | \mathfrak{f}_n^+ \rangle^* \mathfrak{f}_n^-(x), \tag{38}$$

**ADVANCED
SCIENCE NEWS**
www.advancedsciencenews.com

annalen
der **physik**
www.ann-phys.org

while, if $\phi^-(x,0) \in \Phi_-$ then

$$\phi^-(x,t) = \sum_n e^{\gamma(n+1/2)t} \langle \phi^- | \mathfrak{f}_n^- \rangle^* \mathfrak{f}_n^+(x). \tag{39}$$

We stress again that we got an irreversible quantum theory by studying the action of U on $\Phi_\pm$ as a semigroup. Time $t = 0$ splits the evolution in two diametrically opposed directions, and it becomes the instant which separates two different dynamics.

Recalling Eqs. 16 and 17, RHO Gamow eigenstates have the peculiar characteristic of being the quasi-eigenvectors of Fourier transform operator. Indeed, one can observe that the RHO secular equation has the same form as its Fourier transform within a phase factor. Considering the RHO Hamiltonian in the momentum basis ($\hat{p} \to p$ and $\hat{x} \to i\partial_p$) we have:

$$\hat{H}_{RHO}(p, i\partial_p) = \frac{p^2}{2} + \frac{1}{2}\gamma^2 \partial_p^2 = -\hat{H}_{RHO}(-i\partial_x, x). \tag{40}$$

By the way, if one uses this formalism in order to describe a physical experiment, one cannot neglect that GVs have an infinite support, i.e. the x-region where the eigenfunction is not null, is not finite. Hence, to account for the spatial confinement of the experiment, we introduce the windowed Gamow vectors:

$$\phi_G^W(x) = \sum_{n=0}^N \sqrt{\Gamma_n} \mathfrak{f}_n^- \langle \mathfrak{f}_n^+ | \psi(x,0) \rangle \mathrm{rect}_W(x), \tag{41}$$

where $\mathrm{rect}_W(x) = 0$ for $|x| > W$ and $\mathrm{rect}_W(x) = 1$ for $|x| < W$, which is the finite size of the physical system. During the evolution, each Gamow component exponentially decays with rate $\gamma(n+1/2)$: the ground state, i.e. the one with $n = 0$, has the lowest decay rate $\gamma/2$ and higher order Gamow states decay faster than the fundamental one. This allows to consider only the fundamental GV in the long term evolution. We compute the Fourier transform $\mathcal{F}$ of the fundamental state of Eq. (41):

$$\tilde{\psi}(k_x) = \mathcal{F}\left[\mathfrak{f}_0^-(x)\right] = \left(\frac{1}{4} + \frac{i}{4}\right) e^{-\frac{ik_x^2}{2\gamma}} \frac{(-i\gamma\pi)^{1/4}}{W} \times$$

$$\times \left\{ -\mathrm{Erf}\left[\frac{(\frac{1}{2} - \frac{i}{2})(k_x - W\gamma)}{\sqrt{\gamma}}\right] + \right.$$

$$\left. + \mathrm{Erf}\left[\frac{(\frac{1}{2} - \frac{i}{2})(k_x + W\gamma)}{\sqrt{\gamma}}\right] \right\}. \tag{42}$$

This equation will be useful later in the experimental section, Sec. 6.

5. GVs in Nonlocal Nonlinear Optics

In this section, we show that TA-QM formalism models an intrinsically irreversible phenomenon in classical regime, that is, the shock wave propagation in a nonlocal nonlinear medium. Even more, we will see that GVs are able to describe the system long term evolution after the occurrence of the shock point, an unprecedented goal in nonlinear physics. We start from the

paraxial wave equation describing the propagation along the direction Z of an optical beam with complex amplitude $A(\mathbf{R})$, where $\mathbf{R} = (X, Y)$ is the transverse direction, and wavelength λ in a medium with refractive index $n = n_0 + \Delta n[|A|^2](\vec{R})$ and linear loss length L_{loss}:

$$2\iota k \frac{\partial A}{\partial Z} + \nabla_{XY}^2 A + 2k^2 \frac{\Delta n[|A|^2](\vec{R})}{n_0} A = -\iota \frac{k}{L_{loss}} A - \iota \frac{k_2 |A|^2}{L_{loss}} A \tag{43}$$

This equation is called the Nonlinear Schrödinger Equation (NLS), and it is written such that the intensity is $I = |A|^2$, $P_{MKS} = \int I d\mathbf{R}$ is the power and $k = 2\pi n_0/\lambda$ is the wavenumber. It is known in literature that NLS is not Hamiltonian for $\alpha \neq 0$ or $\alpha_2 \neq 0$.[46] In Eq. (43) Δn is the nonlinear nonlocal perturbation to the refractive index

$$\Delta n\left[|A|^2\right](\vec{R}) = n_2 \int G_2(\vec{R} - \vec{R}') I(\vec{R}') d\vec{R}', \tag{44}$$

where n_2 is the nonlinear refractive coefficient and G_2 is the kernel function, normalized such that $\int G_2 d\mathbf{R} = 1$. $G_2 = \delta(\vec{R} - \vec{R}')$ corresponds to the local Kerr effect[47] $G_2 = \delta(\vec{R} - \vec{R}')$. Here we consider a nonlocal medium with an exponential nonlocality function

$$G_2(X, Y) = \exp(-(|X| + |Y|)/L_{nloc})/(2L_{nloc}),$$

where L_{nloc} is the nonlocality length. Being G_2 separable, i.e. $G_2(X, Y) = G_2(X)G_2(Y)$, we can split the equation and consider only the transverse dimension X. For a defocusing nonlinearity, $n_2 < 0$, we write Eq. (43) in terms of dimensionless variables: letting W_0 be the beam waist, we have $x = X/W_0$ and $z = Z/Z_d$, with $Z_d = kW_0^2$ the diffraction length. Equation (43) becomes

$$\iota \frac{\partial \psi}{\partial z} + \frac{1}{2} \frac{\partial^2 \psi}{\partial x^2} - P K(x) * |\psi(x)|^2 \psi = -\iota \frac{\alpha}{2} \psi - \iota \frac{\alpha_2}{2} |\psi|^2 \psi, \tag{45}$$

where $\alpha = Z_d/L_{loss}$, $\alpha_2 = \frac{k_2 Z_d}{k L_{loss}} P_{MKS}$, $\psi = A/\sqrt{P_{MKS}}$ and $\langle \psi | \psi \rangle = 1$. The asterisk $*$ in Eq. (45) represents the convolution integral, while $P = P_{MKS}/P_{REF}$ with $P_{REF} = = \lambda^2/4\pi^2 n_0 |n_2| W_0$, and $K(x) = W_0 G(xW_0) = = \exp(-|x|/\sigma)/2\sigma$ with $\sigma = L_{nloc}/W_0$.

Taking into account a medium where the nonlocality length is much larger than the beam waist, namely, studying a system in the highly nonlocal approximation (HNA), we have[48,49]

$$K * |\psi(x)|^2 \cong \kappa(x),$$

where κ is a function no more depending on $|\psi(x)|^2$, which mimics a delta function in this approximation. For $\alpha = \alpha_2 = 0$ the NLS becomes $\iota\psi_z = \hat{H}\psi$, with the Hamiltonian $\hat{H} = \frac{1}{2}\hat{p}^2 + V(x)$. More precisely, in HNA we can approximate the NLS to a linear Schrödinger equation, being $V(x) = P\kappa(x)$ and $\hat{p} = -i\partial_x$. Having the system an exponential nonlocality, we write the even function κ as its second order expansion, that is, $\kappa(x) = \kappa_0^2 - \frac{\kappa_2^2}{2}x^2$, where $\kappa_0^2 = 1/2\sigma$ and $\kappa_2^2 = 1/\sqrt{\pi}\sigma^2$, thus we have

$$\hat{H} = P\kappa_0^2 + \hat{H}_{RHO}, \tag{46}$$

ADVANCED
SCIENCE NEWS
www.advancedsciencenews.com

annalen
der physik
www.ann-phys.org

where $\hat{H}_{RHO} = \frac{\hat{p}^2}{2} - \frac{\gamma^2\hat{x}^2}{2}$ is the RHO Hamiltonian and $\gamma^2 = P\kappa_2^2$. Consequently, we get GVs

$$|E_n\rangle = \left| E_n^R \pm i\frac{\Gamma_n}{2} \right\rangle,$$

with $E_n^R = P\kappa_0^2$ and $\Gamma_n = \kappa_2\sqrt{P}(2n+1)$. Letting $\psi = \exp(-\iota\kappa_0^2 Pz)\phi$, we obtain $i\phi_z = \hat{H}_{RHO}\phi$.

To summarize, the nonlocal optical propagation in a defocusing medium is a physical realization of a quantum dissipative system,[13] where GVs for the RHO are given by

$$\hat{H}_{RHO}\mathfrak{f}_n^\pm = E_n^\pm \mathfrak{f}_n \tag{47}$$

with purely imaginary eigenvalues $E_n^\pm = \pm\iota\gamma(n+\frac{1}{2})$ and with eigenfunctions[14]

$$\mathfrak{f}_n^\pm(x) = \frac{\sqrt[4]{\pm i\gamma}}{\sqrt{2^n n!\sqrt{\pi}}} H_n(\sqrt{\pm i\gamma}\,x) \exp\left(\mp i\frac{\gamma}{2}x^2\right), \tag{48}$$

being $H_n(x)$ the Hermite polynomials. We have $\hat{H}_{RHO} = \sum_{n=0}^\infty E_n^- |\mathfrak{f}_n^-\rangle\langle\mathfrak{f}_n^+|$, and correspondingly

$$\phi(x) = \phi_N^G(x) + \phi_N^{BG}(x)$$

with

$$\phi_N^G(x) = \sum_{n=0}^N \mathfrak{f}_n^-(x)\langle \mathfrak{f}_n^+|\phi(x,0)\rangle. \tag{49}$$

The evolution of the exponentially decaying part of the wavefunction for $z \geq 0$ is

$$\psi_n^G(x,z) = \sum_{n=0}^N \langle \mathfrak{f}_n^+|\psi(x,0)\rangle \mathfrak{f}_n^-(x) e^{-i\kappa_0^2 Pz} e^{-\frac{\Gamma_n}{2}z}. \tag{50}$$

In the probabilistic interpretation of TA-QM, the projection of Eq. (50) over $\sqrt{\Gamma_n}\mathfrak{f}_n^+$ gives the probability $p_n(z)$ of finding the system in a decaying GV

$$p_n(z) = \Gamma_n \left|\langle \mathfrak{f}_n^+|\psi(x,0)\rangle\right|^2 e^{-\Gamma_n z}, \tag{51}$$

which gives the z-dependent weight of the n-order GV. If $\psi(x,0)$ is a pure GV, $\psi(x,0) = \mathfrak{f}_n^-(x)$, we have $p_n(z) = \Gamma_n \exp(-\Gamma_n z)$, with normalization $\int_0^\infty p_n(z)dz = 1$.[50] The excited GVs have coefficients which depend on the initial profile. For a Gaussian beam $\psi(x,0) = \varphi(x) = \exp(-x^2/2)/\sqrt[4]{\pi}$, all the odd terms in Eq. (50) vanish due the x-parity, and for the first two even GVs we have

$$p_0^G(z) = 2\gamma^{3/2}(1+\gamma^2)^{-1/2}\exp(-\gamma z)$$

and

$$p_2^G(z) = 5\gamma^{3/2}(1+\gamma^2)^{-1/2}\exp(-5\gamma z).$$

We underline that GVs are not decay processes depending on the coupling with the environment (i.e., *extrinsic*), but exponentially decaying states arising from the reversible self-adjoint Hamiltonian (*intrinsic* origin).
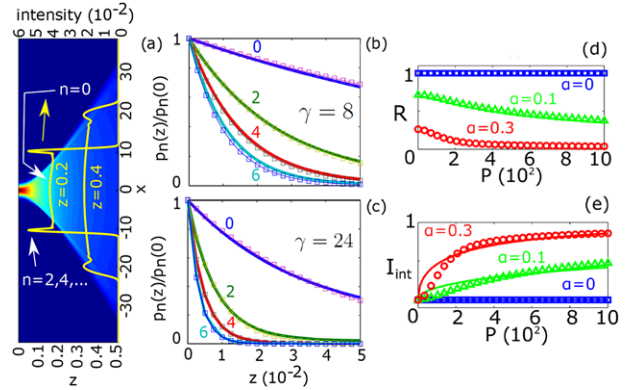

Figure 1. (a) Numerical solution of Eq. (45) with $P = 10^4$ and $\sigma^2 = 10$; (b) projection on GVs for increasing n for $\alpha = 0.3$ and $\gamma = 8$, continuous lines are from Eq. (45), dots are from Eq. (51); (c) as in (b) for $\gamma = 24$; (d) R versus P for various α; (e) intrinsic irreversibility I_{int} for $L = 2, \sigma^2 = 10$, continuous line is after Eq. (54).

To show the occurrence of the GVs in the original nonlinear model, we solve Eq. (45) for $\alpha = \alpha_2 = 0$ with $\psi(x,0) = \varphi(x)$. The evolution of the beam at high power (high wave amplitude) is shown in **Figure 1**a. In correspondence of the DSW, the resulting dynamics clearly displays exponential decays (Figure 1a). At low power (not reported), where the wave breaking is not attained, exponential decays, which describe the intrinsic irreversibility caused by the shock occurence, are not found. The shape of the shock beam strongly resembles the excitation of the ground state GV, corresponding to a central plateau, while lateral tails can be identified with higher order GVs. As the GVs decay exponentially and the power is conserved, the beam displays a self-similar evolution, with an exponential spreading following the classical trajectories of the dissipative system.

To provide quantitative evidence of the presence of $\mathfrak{f}_n^-$, we project at a given z the wavefunction $\psi(x,z)$ over $\mathfrak{f}_n^+$ and retrieve $p_n(z)$ in Eq. (51). Figures 1b,c show $p_n(z)$ decays with quantized rates $\Gamma_n = (2n+1)\gamma$. This trend has been verified for various γ^2 and initial conditions, and confirms the theoretical analysis. The direct evidence of the quantization of decay rates is the most direct signature of GVs, as shown in Figures 1b,c. Deviations from the exact exponential trends are due to finite degree of nonlocality in Eq. (45).

5.1. Gamow Vectors and the Irreversibility of Classical Shock Waves

DSWs are formally reversible, but in real world their reverse process never happens. By the way, in physical experiments there is always an amount of loss. The interplay between linear losses and the excitation of GVs is subtle. In the following, we quantify that irreversibility, in the presence of linear losses, is enhanced by the excitation of GVs. According to the experimental data shown in next section, we neglect the nonlinear losses, because they are not relevant compared to the linear ones, i.e., we consider Eq. (45) with $\alpha > 0$ and $\alpha_2 = 0$.

**ADVANCED
SCIENCE NEWS**

www.advancedsciencenews.com

annalen
der **physik**

www.ann-phys.org

We let $\psi(x, 0) = \varphi(x)$ and retrieve $\psi(x, L)$. We then use the conjugated propagated field as new initial condition $\psi'(x, 0) = \psi(x, L)^*$. As long as the dynamics is reversible, the propagated $\varphi_B(x) = \psi'(x, L)$ coincides with $\varphi(x)$. For $\alpha = 0.3$, reversibility does not occur. The discrepancy between φ and φ_B increases with P, for $\alpha > 0$. Let's introduce the degree of reversibility defined as $R := |\langle \varphi | \varphi_B \rangle|^2$. For a fixed L, R is a function of loss and power, and in the absence of loss $\alpha = 0$, $R(0, P) = 1$ and the dynamics is reversible. For $\alpha > 0$, in the absence of nonlinear effects $P = 0$, R is given by the linear loss $R(\alpha, 0) = \exp(-\alpha L)$. We calculate $R(\alpha, P)$ and, as shown in Figure 1d, the breaking of reversible character appears more pronounced when increasing P for fixed $\alpha > 0$.

To discriminate extrinsic (due to loss $\alpha > 0$) and intrinsic (due to GVs) contribution, we introduce the fraction of the intrinsic irreversibility:

$$I_{int}(\alpha, P) := 1 - \frac{R(\alpha, P)}{R(\alpha, 0)}. \tag{52}$$

$I_{int}(\alpha, P)$ is null if the irreversibility is only due to linear losses, while $I_{int}(\alpha, P) > 0$ quantifies the contribution of the nonlinearity. Figure 1e shows that $I_{int}(\alpha, P)$ grows with P. From the previous discussion we provide an expression for I_{int}. Indeed, at high P the beam is mostly formed by GVs. After forward propagation, letting $L_{eff} = 2(1 - e^{-\alpha L/2})/\alpha$, we have $\psi(x, L) = \mathfrak{f}_n^-(x) \exp[-\alpha L/2 - \Gamma_n(P)L_{eff}/2]$; upon time reversal we have $\psi'(x, 0) = \mathfrak{f}_n^+(x) \exp[-\alpha L/2 - \Gamma_n(P)L_{eff}/2]$, which propagates at a power $P' = P \exp(-\alpha L)$:

$$\varphi_B(x) = \mathfrak{f}_n^+(x) e^{-\alpha L} e^{\left[\Gamma_n(P') - \Gamma_n(P)\right]\frac{L_{eff}}{2}}. \tag{53}$$

By projecting over φ we have for $n = 0$

$$I_{int} = 1 - \exp\left[\kappa_2 \sqrt{P} \left(e^{-\alpha \frac{L}{2}} - 1\right) \frac{L_{eff}}{2}\right], \tag{54}$$

in good agreement with the numerical values in Figure 1d. In the limit of small loss α, Eq. (54) reads as

$$I_{int} = \frac{\sqrt{P}\alpha L^2}{4\sqrt[4]{\pi}\sigma} = \frac{\sqrt[4]{\pi}}{4}\sqrt{\frac{|n_2|I_0}{n_0}} \frac{L_Z^2}{L_{nloc}L_{loss}}, \tag{55}$$

being $I_0 = P_{MKS}/\pi W_0^2$ the peak intensity, and $L_Z = L Z_d$ the propagation length in real world units. The use of GVs radically simplifies the treatment of the highly nonlinear and nonlocal regimes. Eq. (55) shows that the strength of nonlinearity has a direct effect on irreversibility, due to states with intrinsic exponential decay. A small amount of extrinsic loss leads to a breaking of time-reversal that is amplified by nonlinearity.

5.2. Other Intrinsically Irreversible Phenomena in Nonlinear Optics: Thermalization and Self-Organization Processes

The introduction of GVs in studying the irreversible propagation of an optical DSW establishes an important bridge between TA-QM and intrinsically irreversible classical nonlinear phenomena.

When we define the degree of reversibility and the fraction of intrinsic irreversibility, in the previous paragraph, we use common tools of QM. We consider a wave at the final instant of its evolution and make it propagate backward. Then we compute specific bra-ket products. As a matter of fact, we did not switch to a statistical picture because this system is an analytically solvable eigenvalue problem.

For the sake of completeness, we highlight that nonlinear optics offers other examples of intrinsical irreversibility, most of them studied by statistical approach. In particular, we mention the dynamics of incoherent nonlinear optical waves, in which the statistical interpretation has produced significative results. Statistical nonlinear optics is related to wave turbulence theory, whereby the kinetic wave description provides a thermodynamic treatment of turbulence. If one considers the nonlinear propagation of partially coherent optical waves characterized by fluctuations that are statistically homogeneous in space, one can see that the optical field evolves towards thermodynamic equilibrium. In weakly nonlinear system, the description of the field evolution is deeply studied in Ref. [51]. This analysis points out a different kind of time asymmetric behavior with respect to DSWs reported above, because SWs arise only in the strong turbulence regime,[52] where dispersive shock waves have been shown to emerge from a turbulent field.

A convenient way of interpreting the results of the multi-scale expansion in weak turbulence is the so-called "random phase approximation", which may be considered as justified when phase information becomes irrelevant. The random phases can thus be averaged in order to obtain a weak turbulence description of the wave interaction. It results that, even if the equation governing wave propagation is formally reversible, the kinetic equation describes an irreversible evolution of the field to thermodynamic equilibrium, i.e., the fundamental Rayleigh-Jeans spectrum. The mathematical statement of such irreversibility relies on the H-theorem of entropy growth. Wave thermalization can be characterized by a self-organization process, that is, the system spontaneously generates a large-scale coherent structure. A remarkable example of this self-organization process is the wave condensation, whose thermodynamic equilibrium properties are similar to those of quantum Bose-Einstein condensation. A detailed treatise of these phenomena is reported in Ref. [51] and in the references therein.

6. Experimental Results

In this section we report on two experiments which show the presence of GVs in DSWs and prove the power of this formalism in the description of the shock phenomenon. In order to validate the theoretical analysis previously exposed, we excited a shock wave in a nonlinear nonlocal optothermal medium. In this way we could generate a quantized inverted oscillator. The heat diffusion in the photothermal liquid, belonging to the presence of the intense laser beam in the sample, causes the extension of the refractive index perturbation far beyond the beam intensity profile.[48,53–55] Hence, light experiences a refractive index with an inverted parabolic spatial distribution.[48,56,57] We remark that the presence of nonlinearity in the system gives us the possibility to
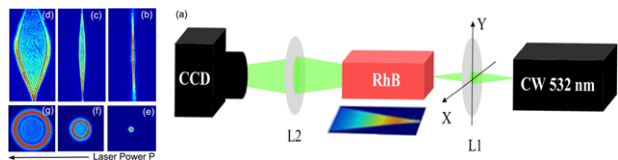
**ADVANCED
SCIENCE NEWS**

www.advancedsciencenews.com

annalen
der **physik**

www.ann-phys.org

Figure 2. (a) Experimental setup to collect the transmitted and top fluorescence images of the laser beam propagating in the RhB samples. We used two types of launching lenses L1: cylindrical and spherical in order to obtain the 1D and 2D experiments respectively. The top fluorescence image of the propagating beam was collected by a microscope (not shown) placed above the RhB sample. L2 is the spherical lens used to collect the transmitted beam at the exit face of the sample. (b-g) Transmitted images as obtained in 1D (b-d) and 2D experiments for increasing laser power, P.

distinguish GVs from linear losses, which are not included in the RHO model.

In **Figure 2**a we illustrate the experimental setup and the top-view imaging apparatus for the two experiments. A continuous wave (CW) laser beam at 532 nm wavelength is focused through a lens (L1) into a sample. The light is collected by a spherical lens (L2) and a Charged Coupled Device (CCD) camera. A microscope is placed above the sample in order to capture top-view images of the laser beam along the propagation direction Z. Samples are prepared by dispersing 0.1 mM of Rhodamine B in water. The solution is placed in a cuvette 1 mm thick in the propagation direction. The measured defocusing Kerr coefficient is $|n_2| = 2 \times 10^{-12} \mathrm{m^2 W^{-1}}$ and the absorption length $\mathrm{L}_{abs} \simeq 1.6$ mm at the laser wavelength.[35]

The difference between the two experimental apparatus is the choice of the first lens (L1). In the first experiment, we used a cylindrical lens (L1) with focal length $f = 20$ cm in order to mimic a nearly one-dimensional propagation. Being Z the propagation direction, the lens focuses the beam in the X direction. The spot dimension is 1.0 mm in the Y direction and 35 μm in the X direction. These geometrical features make the one-dimensional approximation valid and allow to compare experimental results with the theoretical one-dimensional model. The diffraction length in the X direction is $L_{diff} = 3.0$ mm. Otherwise, in the second experiment, the lens (L1) is spherical with focal length 100mm, with a focus spot size of 10 μm. This time the setup was placed having the beam propagating vertically through the sample, reducing convection in the water.

In Figure 2b–g we report the CCD transmitted images obtained in the 1D (b–d) and 2D(e–g) experimental configurations for increasing laser powers P. The beam displays a strongly divergent funnel shape, the signature of optical nonlinearity in the RhB solution. At low powers, beam propagation does not manifest the strong divergence and is dominated by diffraction.[35]

6.1. One-Dimensional Experiment

As stated above, the RHO eigenstates are quasi-eigenstates of the Fourier transform operator, which in optics gives us the form of the far field. Hence, Eq. (42) provides an analytical expression of the far field, which is compared below with the experiments (**Figure 3**). Indeed, Eq. (42) allows to predict in closed form the typical shock "M-shape" profile: it describes the internal undu-
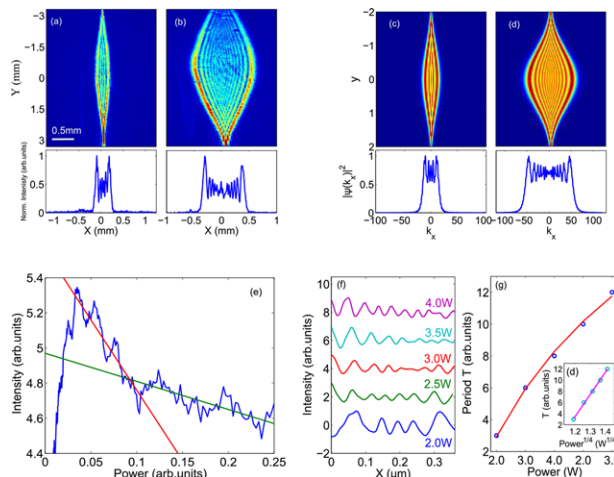

Figure 3. (a-b) CCD image of the light beam at laser powers $P_{MKS} = 2$W and 4W respectively; the bottom panels show the normalized intensity profile at the maximum waist along $Y = 0$. (c) Analytical solution obtained by Eq. (42) changing Gaussianly the power P in the y direction. (d) As in (c) but for higher powers; the bottom panels show the slice of panel (c) and (d) at $y = 0$, i.e. Eq. (42) square modulus for $W = 1.5$ and $\gamma \simeq 12$ and $\gamma \simeq 40$, respectively. (e) Log-scale normalized intensity as a function of power as obtained by slicing along Y a region in panel (b). The slopes of the straight lines give the Gamow vectors decay rates ($\gamma_1 = -8 \pm 0.4$ and $\gamma_2 = -1.6 \pm 0.1$). Their quantized ratio is 5.0 ± 0.4 as expected from theory (see[17]). The units of axes in panel (e) correspond to scaled X and Y direction in panel (a). (f) Intensity oscillations for different power values. (g) Measured oscillations period T as a function of power; continuous line is the fit function $T \propto \sqrt[4]{P}$ as expected by the theory; the inset show the same curve of (g) with $P_{MKS}^{1/4}$ as abscissa axis.

lar bores and the correct scaling of the undulation period with respect to the power, i.e. the period T is predicted to scale with the square root of γ, and hence with the forth square root of the beam input power.

The "M-shape" profile of SWs has been shown in Ref. [52] as well. There, it is theoretically predicted (and then experimentally proved) that nonlocal NLS equation solutions exhibit a collapse singularity for the intensity, developed on the boundary of the optical beam. This singularity originates exactly in the nonlocal nonlinearity, since the corresponding hydrodynamic equations in the limit of a local nonlinearity recover the shallow water equations, which are known to exhibit the pure shock singularity without the collapse.

We collect CCD images of the beam in the far field (corresponding to the square modulus of the spatial intensity Fourier transform of the beam) for different input powers. The investigated power range is from 0W to 4W (Figure 3). For low power ($P_{MKS} \leq 1$W) the elliptical beam profile remains Gaussian along propagation (see Figure 2b). Instead, while increasing the power, the beam transverse X section broadens (Figures 2c–d with $P = 2W$ and 4W respectively and Figures 3a–b) and the beam develops intensity peaks ("M-shape" profile) on its lateral edges (bottom panels of Figures 3a–b). The bottom panels of Figures 3a–b show the intensity profile at $Y = 0$. These results are in remarkable agreement with Eq. (42) as shown in Figures 3c–d. Indeed, Figures 3c–d are obtained from the square modulus of Eq. (42). Different positions in the y direction correspond to
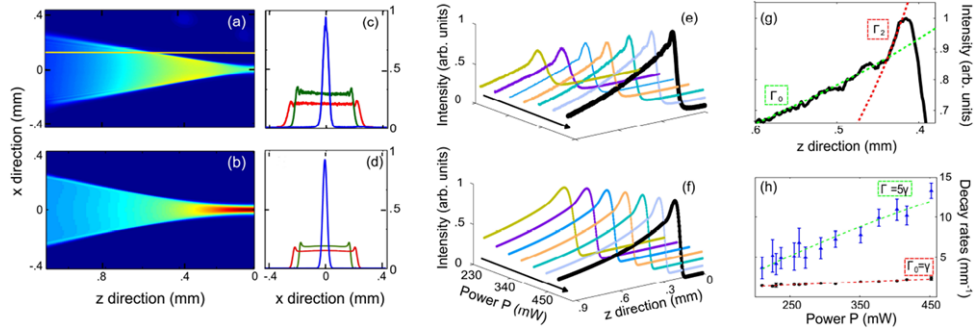
Figure 4. (a-b) Top-view intensity distribution as obtained from 2D experiment (a) and numerical simulations (b). Respectively experimental (c) and numerical (d) sections of the images (a) and (b) taken at $z = 0.2$, 0.6 and 0.9mm. (e) Observed intensity decay at different laser powers as obtained by slicing along the propagation direction the top-view intensity distribution (see the yellow line in panel (a)). (f) Numerically calculated decays in the conditions of panel (e). (g) Enlargement of the peak region of the experimental curve at $P = 450$mW. The double exponential decay unveils the existence of two exploding states, the fundamental state, $n = 0$ (slow decay) and the excited state, $n = 2$ (fast decay). (h) Decay rates vs P for the fundamental state, Γ_0 (filled circles) and the excited state, Γ_2, (triangles).

different power levels. Any power level furnishes a different value of γ, being $\gamma = \sqrt{P/\sqrt{\pi}\sigma^2}$. The Gaussian beam profile in the y direction $P \propto exp(-y^2)$ provides the link between y and P and γ. The bottom panels of Figures 3c–d correspond to $\gamma = 12$ and $\gamma = 40$.

We remark that the experimental CCD images display the characteristic undular bores of the shock that appear between the lateral peaks, in the internal part of the Gaussian beam. This is also found in the analytical solution (bottom panel of Figures 3c–d). We also observe that the experimental data (bottom of Figures 3a–b) exhibit a reduction in the central part of the profile. This is mostly caused by the presence of nonlinear losses ($\beta_2 \simeq 10^{-5}$ m/W − not included in the model): the thermal effect induces Rhodamine diffusion out of the highest intensity regions, which, in turn, are hence subject to a reduced absorption.[25]

Exponential decays are the major signature of Gamow states.[16–19] As discussed above, the elliptical beam has an intensity that varies Gaussianly along Y. This implies that, observing a CCD image, intensity profiles at different Y correspond to different powers; the link between the Y position and the power follows the Gaussian profile ($P_{MKS} \propto \exp -Y^2/Y_0^2$), where Y_0 is the vertical beam waist ($Y_0 \simeq 3$ mm). Correspondingly, the expected exponential trend with respect to the power can be extracted from a single picture by looking at different Y positions. Indeed, different y means a different P, and hence a different γ. If the decay rate is quantized, which is predicted by the Gamow theory, this quantization affects the beam intensity along y.

Exponential decays are extracted considering a region in the up panel of Figure 3b; the resulting profile versus power is shown in Figure 3e: two exponential trends are clearly evident and the two straight lines corresponding to different decay coefficients are drawn (the conversion from Y to P_{MKS} correspond to a logarithmic scale in which exponentials are straight lines). The extracted ratio of the two decay coefficients is 5 and hence in agreement with the expected quantized theoretical value.[17]

We analyze the undular bores of shock waves (see Figures 3f–g). As said before, Eq. (42) predicts that the field intensity undulation period T grows like $T \propto \sqrt[4]{P}$.

We performed a spectral analysis of the oscillations extracted from the CCD images collected removing the second lens (L2)

for different injected power P_{MKS} (see Figure 3f). Taking the oscillations in the X-direction at the maximum waist along Y we normalize the intensity oscillations and analyze them by a sinusoidal fit. Figure 3f shows the intensity oscillations. Data have been shifted on the axes to allow a clearer view of the oscillations. By spectral analysis we extract the period as a function of the input optical power (Figure 3g). In order to demonstrate univocally the period's $\sqrt[4]{P}$ trend, we report the period T as function of $\sqrt[4]{P}$ (abscissa axes). As shown in the inset of Figure 3g, we obtain a linear behavior which is in agreement with our theory.

6.2. Two-Dimensional Experiment

In order to further validate the theoretical analysis we made a 2-dimensional experiment through which clearly observe GVs decay rates, Γ_n.

Decay rates are detected by slicing the intensity profile $I(x, z)$ at $x \simeq 0.1$ mm and fitting the intensity versus z data with two exponential functions. The analysis is repeated for different samples and at different power levels. **Figure 4**a reports the observed laser beam propagation and Figure 4b the numerical calculation from the propagation equation. The beam displays the characteristic strongly divergent shape, signature of optical shock in nonlinear media at high power.

The comparison between the experimental and numerical features of the $\mathfrak{f}_n^-$ eigenstates are reported in Figures 4c–d, where three transverse sections of the intensity profile at different propagation distances $z = 0.2$, 0.6 and 0.9 mm are displayed. The observation of quantized decay rates is reported in panels e-h of Figure 4. The decay dynamics at different power levels, shown in Figures 4e–f, are obtained by slicing the intensity profile along the propagation z-direction (see yellow line in Figure 4a). The signature double exponential behavior is most evident at high power (Figure 4e). Observed and calculated double-exponential decay dynamics are found to obey the quantized spectrum scaling $\Gamma_2/\Gamma_0 = 5$ at all investigated power levels, P (Figure 4g). This demonstrates that we excite the fundamental state ($\mathfrak{f}_0^-$, n= 0) and the first excited state ($\mathfrak{f}_2^-$, $n = 2$). The state $\mathfrak{f}_1^-$ is not excited, as expected from the input beam symmetry. Each of the two rates is found to have a square

ADVANCED
SCIENCE NEWS

www.advancedsciencenews.com

annalen
der **physik**

www.ann-phys.org

root dependence on P (see the superimposed dashed lines in Figure 4g), signature of the underlying nonlinearity. This power dependence distinguishes RHO dynamics from linear loss, due to absorption and scattering.

In this way we proved that RHS Hamiltonian theories are able to describe irreversible processes and include the arrow of time as originating from dynamics, as opposed to the commonly accepted statistical origin. Light beams in photothermal liquids provide direct evidence of the main prediction of the theories: the existence of physical processes that manifest discrete decay rates.

7. Conclusions

We reviewed the formulation of quantum mechanics in the rigged Hilbert space from a mathematical point of view, most of all by analyzing the paradigmatic model of the reversed harmonic oscillator. We considered the time asymmetric evolution of a wavefunction by a superposition of Gamow vectors and studied in which function spaces the evolution operator acts as a semigroup.

We applied the theory to the specific case of dispersive shock waves in a nonlocal medium. We illustrated that these phenomena are driven by the nonlinear Schrödinger equation and that this equation can be approximated to a quantum reversed harmonic oscillator system, with imaginary frequency (and related Gamow vectors) depending on the square root of the power. This feature allows to distinguish between the intrinsic irreversibility and the extrinsic losses, hence we quantitatively measured the degree of irreversibility of the nonlinear shock.

We demonstrated these theoretical achievements in two different experiments. The first one confirmed that dispersive shock waves can be analyzed by the reversed harmonic oscillator, and that Gamow vectors describe the wave propagation beyond the shock point explaining the M-shape shock profile. The second one showed and undoubtful validation of the presence of quantized decay rates in the shock propagation distinguishing the GVs decay rated from linear losses.

This review has the aim of leading the reader into the theoretical and experimental work made by the authors in the last three years about the description of DSWs by TA-QM. For a further study, one can see[16] for the formalism,[17] for the theoretical part regarding the link between nonlinear optics and the TA-QM, and[18,19] for the experiments.

We believe that our results address some of the known concepts of the RHS approach to the dynamics of unstable systems and that Gamow vectors may also open novel possibilities in studying extreme irreversible classical and quantum systems.

Appendix A

This appendix is written to let the reader find the mathematical definitions used in Sec. 2 quickly. It presents only a list of definitions, without any ambition to explain the mathematics that is behind. For more details, one can see.[40–43]

Definition 8.1. *Given a set X, a **topology** τ is a collection of elements of the power set $P(X)$ such that:*

– $\emptyset, X \in \tau$;
– $\cup_{n=1}^{\infty} A_n \in \tau \ \forall \{A_n\}_{n \in \mathbb{N}} \subset \tau$;
– $\cup_{n=1}^{N} A_n \in \tau \ \forall \{A_1, ..., A_N\} \subset \tau$.

*The members of τ are called **open sets**.*

Definition 8.2. *Given two topologies τ_1 and τ_2 on the same set X, we say that τ_1 is **finer** or **stronger** than τ_2 if $\tau_2 \subset \tau_1$.*

Definition 8.3. *Let $f : X \rightarrow Y$ be a function between two topological spaces (X, τ_X) and (Y, τ_Y). f is said to be **continuous** if and only if*

$$f^{-1}(A) \in \tau_X \ \forall A \in \tau_Y.$$

Definition 8.4. *Let $f : X \rightarrow Y$ be a function between two topological spaces (X, τ_X) and (Y, τ_Y). f is called a **homeomorphism** if and only if f is a bijective continuous function with continuous inverse function.*

Definition 8.5. *Let (X, τ) be a vector space with a topology τ. If τ makes the vector addition and the scalar multiplication be continuous on X, then we say that (X, τ) is a **topological vector space**.*

Definition 8.6. *A subset $\mathcal{B}$ of the topology τ is a **basis** (or a **base**) of τ if*

$$\forall A \in \tau \ \exists \{B_i\}_{i \in I \subseteq \mathbb{N}} \subset \mathcal{B} \ | \ A = \cup_{i \in I} B_i.$$

Definition 8.7. *Given $x \in X$, a **neighborhood** U of x is a subset of X such that $\exists A \in \tau \ | \ x \in A \subseteq U$.*

Definition 8.8. *Given $x \in X$ and given the neighborhood system centered at x*

$$I(x) = \{U \subseteq X \ | \ U \text{ is a neighbourhood of } x\},$$

*a **neighborhood local basis** is a subset J of $I(x)$ such that $\forall U \in I(x) \ \exists A \in J \ | \ A \subset U.$*

Definition 8.9. *A topological space (X, τ) is a **Hausdorff space** if*

$$\forall x, y \in X \ \exists U \in I(x), V \in I(y) \ | \ U \cap V = \emptyset.$$

Definition 8.10. *Let (X, τ) be a topological vector space. A subset C of X is said to be **convex** if the segments $\{(1 - t)x + ty \ | \ 0 \leq t \leq 1\}$ are contained in C for any $x, y \in C$.*

Definition 8.11. *Let (X, τ) be a topological vector space. (X, τ) is said to be **locally convex** if $\mathcal{C} = \{C \in I(0) \ | \ C \text{ is convex}\}$ is a neighborhood local basis.*

Definition 8.12. *Let $\{\psi_n\}_{n \in \mathbb{N}}$ be a sequence of elements of X, where (X, τ) is a topological vector space. Let $\mathcal{B}$ be a neighborhood local basis that is centered at 0. $\{\psi_n\}_{n \in \mathbb{N}}$ is said to be a **Cauchy sequence** if*

$$\forall B \in \mathcal{B} \ \exists \nu \in \mathbb{N} \ | \ \phi_m - \phi_n \in B \ \forall m, n > \nu.$$

Definition 8.13. *A topological vector space is said to be **complete** when it contains the limit elements of every its Cauchy sequence.*

Definition 8.14. *Let (X, τ) be a topological vector space. A topological vector space Y is the X **completion** according to τ if it is the smallest vector space that contains every members of X and each limit element of Cauchy sequences in X.*

**ADVANCED
SCIENCE NEWS**

www.advancedsciencenews.com

annalen
der **physik**

www.ann-phys.org

Definition 8.15. *Let X be a set. A **metric** (or a **distance**) on X is a function $d : X \times X \to \mathbb{R}$ that satisfies the following three conditions:*

- $d(x, y) \geq 0 \ \forall x, y \in X$ and $d(x, y) = 0 \Leftrightarrow x = y$;
- $d(x, y) = d(y, x) \ \forall x, y \in X$;
- $d(x, z) \leq d(x, y) + d(y, z) \ \forall x, y, z \in X$.

Definition 8.16. *Given a metric space (X, d), we define an **open ball** of radius $r \in \mathbb{R}^+$ centered at $x_0 \in X$ as the set*

$$B_r(x_0) = \{x \in X \mid d(x_0, x) < r\}.$$

Definition 8.17. *Let (X, d) be a metric space. d induces a **metric topology** τ_d on X, which is generated by the basis $\mathcal{B} = \{B_r(x) \mid x \in X, \ r \in \mathbb{R}^+\}$. In τ_d, the subset $J = \{B_r(0) \mid r \in \mathbb{R}^+\}$ of $\mathcal{B}$ is a neighborhood centered at the origin.*

Definition 8.18. *Let X be a set. A **norm** on X is a function $\|\cdot\| : X \to \mathbb{R}$ that satisfies the following three conditions:*

- $\|x\| \geq 0 \ \forall x \in X$ and $\|x\| = 0 \Leftrightarrow x = 0$;
- $\|ax\| = |a| \ \|x\| \ \forall x \in X, \ \forall$ scalar a;
- $\|x + y\| \leq \|x\| + \|y\| \ \forall x, y \in X$.

Definition 8.19. *In a topological space (X, τ), a point $x_0 \in X$ is the **limit** of the sequence $\{x_n\}_{n \in \mathbb{N}}$ if*

$$\forall U \in I(x_0) \ \exists \nu \in \mathbb{N} \mid x_n \in U \ \forall n > \nu.$$

Definition 8.20. *$A \subset X$ is **dense** in (X, τ) if every point $x \in X$ either belongs to A or is a limit point of a sequence in A.*

Definition 8.21. *A topological vector space that is normed and complete with respect to the norm is called **Banach space**.*

Definition 8.22. *A topological vector space with a scalar product is called **Euclidean space**.*

Definition 8.23. *A Banach space with a scalar product is called **Hilbert space**.*

Definition 8.24. *Given a set X, an **algebra** $\mathcal{A}$ is a collection of elements of the power set $P(X)$ such that:*

- $\emptyset \in \mathcal{A}$;
- $A^c \in \mathcal{A} \ \forall A \in \mathcal{A}$;
- $A \cup B \in \mathcal{A} \ \forall A, B \in \mathcal{A}$.

Definition 8.25. *Given a set X, a σ-**algebra** $\mathcal{A}$ is a collection of elements of the power set $P(X)$ such that:*

- $\emptyset \in \mathcal{A}$;
- $A^c \in \mathcal{A} \ \forall A \in \mathcal{A}$;
- $\cup_{n=1}^{\infty} A_n \in \mathcal{A} \ \forall \{A_n\}_{n \in \mathbb{N}} \subset \mathcal{A}$.

*The members of $\mathcal{A}$ are called **measurable sets**.*

Remark 8.1. *Each σ-algebra is an algebra.*

Definition 8.26. *Given an algebra $\mathcal{A}$, a **measure** on $\mathcal{A}$ is a function $\mu : \mathcal{A} \to \bar{\mathbb{R}}$ that satisfies the following three conditions:*

- $\mu(\emptyset) = 0$;
- $\mu(A) \geq 0 \ \forall A \in \mathcal{A}$;
- $\mu(\cup_{n=1}^{\infty} A_n) = \sum_{n=1}^{\infty} \mu(A_n) \ \forall \{A_n\}_{n \in \mathbb{N}} \subset \mathcal{A} \mid \cup_{n=1}^{\infty} A_n \subset (A), \quad A_k \cap A_j = \emptyset \ \forall k \neq j$.

Definition 8.27. *Given a set X, an algebra $\mathcal{A}$ on X and a measure μ on $\mathcal{A}$, a **measure space** is the triplet $(X, \mathcal{A}, \mu)$.*

Definition 8.28. *Let $(X, \mathcal{A}, \mu)$ be a measure space. If $\mu(X) = 1$, $(X, \mathcal{A}, \mu)$ is a **probability space** and μ is called a **probability measure**.*

Definition 8.29. *Given a vector space V on a field $\mathbb{K}$, $V^* = \{F : V \to \mathbb{K} \mid F \text{ is continuous and linear}\}$ is called a **dual space** of V, and any $F \in V^*$ is called a **linear functional**. Moreover, if W is a vector subspace of V, then $V^* \subset W^*$.*

The one which follows is a fundamental theorem about the representation of the dual space of a Hilbert space.

Theorem 8.1 Riesz-Fréchet. *Let $\mathcal{H}$ be a Hilbert space. Given any $F \in \mathcal{H}^*$, there exists a unique $f \in \mathcal{H}$ such that*

$$\langle F | \phi \rangle = (f | \phi) \ \forall \phi \in \mathcal{H},$$

where $\langle F | \phi \rangle := F(\phi)$ is the operatorial product. Moreover,

$$\|F\|_{\mathcal{H}^*} = \sup_{\|\phi\|_{\mathcal{H}} \leq 1} |\langle F | \phi \rangle| = \|f\|_{\mathcal{H}}.$$

Definition 8.30. *Let us consider a continuous linear operator $A : \mathcal{H} \to \mathcal{H}$, where $\mathcal{H}$ is a Hilbert space. Then the **adjoint** of A is the continuous linear operator $A^\dagger : \mathcal{H} \to \mathcal{H}$ satisfying*

$$(Ax | y) = (x | A^\dagger y) \ \forall x, y \in H.$$

*If $A = A^\dagger$ it is a **Hermitian** (or **self-adjoint**) operator. Moreover, if A is a Hermitian continuous operator, its spectrum is real.*

Definition 8.31. *A continuous linear operator $U : \mathcal{H} \to \mathcal{H}$ is said to be **unitary** if and only if $U^\dagger = U^{-1}$. Moreover, an operator U is unitary on $\mathcal{H}$ if and only if U is an isometry, i.e. $\|Ux\| = \|x\|$.*

Definition 8.32. *Let us define the **Hardy space** $\mathcal{H}^p_+$ ($\mathcal{H}^p_-$), $p \in (0; +\infty)$ for the upper half space (for the lower half space) as the space of the holomorphic functions $f : \mathbb{C} \to \mathbb{C}$ such that $\|f\| := \sup_{y>0}[\int_{\mathbb{R}} |f|]^{1/p}$ ($\|f\| := \sup_{y<0}[\int_{\mathbb{R}} |f|]^{1/p}$) is a finite real number.*

Acknowledgements

Conflict of Interest

The authors delcare no conflict of interest.

Keywords

[1] G. Gamow *Z. Phys.* **51**, 204 (1928).
[2] G. Gamow *Nature* **122**, 805 (1928).
[3] I. Prigogine, F. Mayné, C. George, and M. D. Haan *Proc. Natl. Acad. Sci. USA* **74**, 4152 (1977).
[4] A. Bohm *J. Math. Phys.* **22**(12), 2813–2823 (1981).
[5] A. Bohm, M. Gadella, and G. B. Mainland *Am. J. Phys.* **57**, 1103 (1989).
[6] I. E. Antoniou and I. Prigogine *Physica A* **192**, 443 (1993).
[7] M. Castagnino, R. Diener, L. Lara, and G. Puccini *Int. Jour. Theo. Phys.* **36**, 2349 (1997).
[8] A. Bohm and N. L. Harshman *Lectures Notes in Phys.* **504**, 179 (1998).
[9] A. Bohm *Phys. Rev.* **A60**, 861 (1999).
[10] A. R. Bohm, R. Scurek, and S. Wickramasekara, Resonances, Gamow vectors and time asymmetric quantum theory, in: 22nd Symposium on Nuclear Physics Oaxtepec, Morelos, Mexico, (1999).
[11] R. de la Madrid and M. Gadella *Am. J. Phys.* **70**, 626 (2002).
[12] D. Chruściński *Open Sys. Information Dyn.* **9**, 207–221 (2002).
[13] D. Chruściński *J. Math. Phys.* **44**, 3718–3733 (2003).
[14] D. Chruściński *J. Math. Phys.* **45**, 841 (2004).
[15] O. Civitarese and M. Gadella *Phys. Rep.* **396**, 41 (2004).
[16] G. Marcucci and C. Conti *Phys. Rev. A* **94**, 052136 (2016).
[17] S. Gentilini, M. C. Braidotti, G. Marcucci, E. DelRe, and C. Conti *Phys. Rev. A* **92**, 023801 (2015).
[18] S. Gentilini, M. C. Braidotti, G. Marcucci, E. DelRe, and C. Conti *Sci. Rep.* **5**, 15816 (2015).
[19] M. C. Braidotti, S. Gentilini, and C. Conti *Opt. Express* **24**(19), 21963–21970 (2016).
[20] S. Longhi and S. M. Eaton *Opt. Lett.* **41**, 1712 (2016).
[21] A. Gleason *J. Math. and Mech.* **6**(6), 885 (1957).
[22] M. H. Stone *Ann. of Math.* **33**(3), 643 (1932).
[23] G. C. Hegerfeldt *Phys. Rev. Lett.* **72**, 596 (1994).
[24] L. A. Khalfin *Sov. Phys. JETP* **6**, 1053 (1958).
[25] S. Gentilini, N. Ghofraniha, E. DelRe, and C. Conti *Phys. Rev. A* **87**, 053811 (2013).
[26] M. A. Hoefer, M. J. Ablowitz, I. Coddington, E. A. Cornell, P. Engels, and V. Schweikhard *Phys. Rev. A* **74**, 023623 (2006).
[27] A. Fratalocchi, A. Armaroli, and S. Trillo *Phys. Rev. A* **83**, 053846 (2011).
[28] J. Garnier, G. Xu, S. Trillo, and A. Picozzi *Phys. Rev. Lett.* **111**, 113902 (2013).
[29] S. Gentilini, F. Ghajeri, N. Ghofraniha, A. D. Falco, and C. Conti *Opt. Express* **22**(2), 1667–1672 (2014).
[30] C. Lecaplain, J. M. Soto-Crespo, P. Grelu, and C. Conti *Opt. Lett.* **39**(2), 263–266 (2014).
[31] A. Moro and S. Trillo *Phys. Rev. E* **89**, 023202 (2014).
[32] G. B. Whitham, *Linear and Nonlinear Waves* (Wiley, New York, 1999).
[33] W. Wan, S. Jia, and J. W. Fleischer *Nat. Phys.* **3**(1), 46–51 (2007).
[34] N. Ghofraniha, C. Conti, G. Ruocco, and S. Trillo *Phys. Rev. Lett.* **99**(4), 043903 (2007).
[35] N. Ghofraniha, S. Gentilini, V. Folli, E. DelRe, and C. Conti *Phys. Rev. Lett.* **109**, 243902 (2012).
[36] U. G. Aglietti and P. M. Santini *Phys. Rev. A* **89**, 022111 (2014).
[37] M. Crosta, S. Trillo, and A. Fratalocchi *New Journal of Physics* **14**(9), 093019 (2012).
[38] A. V. Gurevich and L. Pitaevskii *Sov. Phys. JETP* **38**, 291 (1974).
[39] G. A. El, A. Gammal, E. G. Khamis, R. A. Kraenkel, and A. M. Kamchatnov *Phys. Rev. A* **76**, 053813 (2007).
[40] H. Brezis, *Functional Analysis, Sobolev Spaces and Partial Differential Equations* (Springer, 2010).
[41] J. R. Munkres, *Topology*, second edition (Prentice Hall, Inc., 2000).
[42] H. L. Royden, *Real Analysis*, third edition (Macmillan Publishing Company, 1988).
[43] W. Rudin, *Real and Complex Analysis*, 3rd edition (McGraw-Hill, Inc., 1987).
[44] M. Gadella and F. Gomez *Int. J. Theor. Phys* **42**(10), 2225 (2003).
[45] G. Barton *Ann. Phys.* **166**, 322 (1986).
[46] M. Lisak, B. A. Malomed, and D. Anderson *Opt. Lett.* **16**(24), 1936–1937 (1991).
[47] R. W. Boyd, *Nonlinear Optics*, 3rd edition (Academic Press, 2008).
[48] A. W. Snyder and D. J. Mitchell *Science* **276**, 1538–1541 (1997).
[49] V. Folli and C. Conti *Opt. Lett.* **37**(3), 332–334 (2012).
[50] T. Shimbori and T. Kobayashi *Nuovo Cim. B* **115**, 325–342 (2000).
[51] A. Picozzi, J. Garnier, T. Hansson, P. Suret, S. Randoux, G. Millot, and D. Christodoulides *Phys. Rep.* **542**(1), 1–132 (2014).
[52] G. Xu, D. Vocke, D. Faccio, J. Garnier, T. Roger, S. Trillo, and A. Picozzi *Nat. Commun.* **6**, 8131 (2015).
[53] O. Bang, W. Krolikowski, J. Wyller, and J. J. Rasmussen *Physical Review E* **66**, 046619 (2002).
[54] S. K. Turitsyn *Teor. Mat. Fiz.* **64**, 226 (1985).
[55] C. Rotschild, O. Cohen, O. Manela, M. Segev, and T. Carmon *Physical Review Letters* **95**(21), 213904 (2005).
[56] J. P. Gordon, R. C. C. Leite, R. S. Moore, S. P. S. Porto, and J. R. Whinnery *Journal of Applied Physics* **36**(1), 3–8 (1965).
[57] C. Conti, M. Peccianti, and G. Assanto *Phys. Rev. Lett.* **92**(Mar), 113902 (2004).